UNIVERSITAT DE BARCELONA

B:KC Barcelona Knowledge Campus

Institut de Ciències del Cosmos

Recent results from NPLQCD

Assumpta Parreño (U Barcelona)

for the NPLQCD Collaboration

nplqcd.ub.edu

EMMI Workshop: Anti-matter, hyper-matter and exotica production at the LHC

Nov. 6-10, 2017@Torino

Beane *Davoudi* *Orginos* *Savage* *Tiburzi* *Winter*

Chang *Detmold* *Parreño* *Shanahan* *Wagman*

NPLQCD Phys. Rev. D87 (2013) 3, 034506

$SU(3)_f$

$m_\pi \sim 800$ MeV

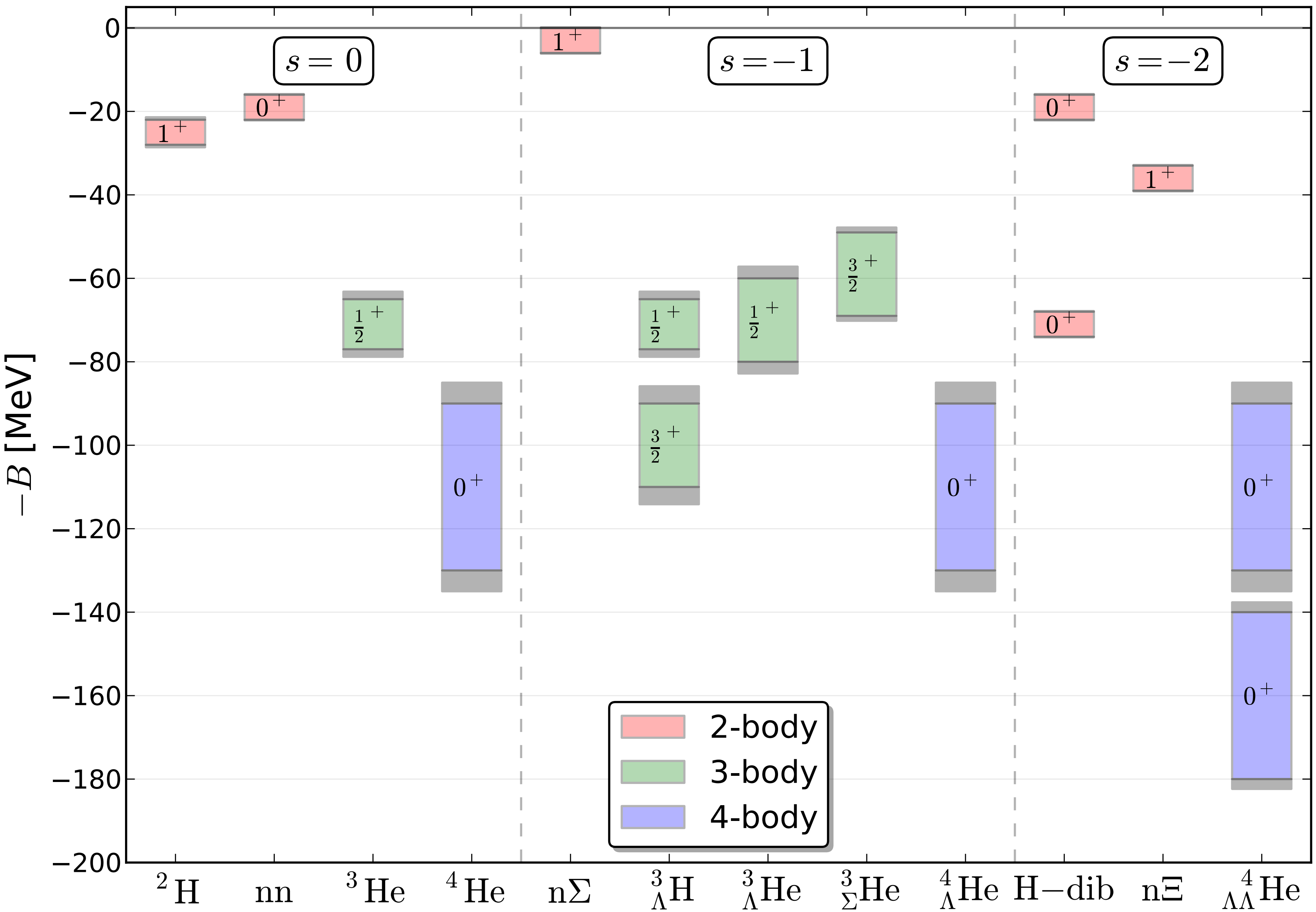

no e.m. interactions

(hadronic labels for (J^π, I, s, A) states)

Two-baryon states

SU(3) decomposition

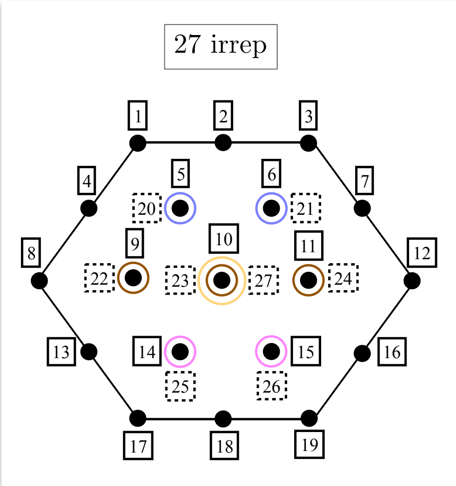

	Flavor channel		Flavor channel
1	nn	14	$-\sqrt{\frac{2}{3}}\Sigma^0\Xi^- + \sqrt{\frac{1}{3}}\Sigma^-\Xi^0$
2	$\frac{1}{\sqrt{2}}(np+pn)$	15	$\sqrt{\frac{1}{3}}\Sigma^+\Xi^- + \sqrt{\frac{2}{3}}\Sigma^0\Xi^0$
3	pp	16	$\Sigma^+\Xi^0$
4	$\Sigma^- n$	17	$\Xi^-\Xi^-$
5	$\sqrt{\frac{2}{3}}\Sigma^0 n + \sqrt{\frac{1}{3}}\Sigma^- p$	18	$\frac{1}{\sqrt{2}}(\Xi^-\Xi^0 + \Xi^0\Xi^-)$
6	$-\sqrt{\frac{1}{3}}\Sigma^+ n + \sqrt{\frac{2}{3}}\Sigma^0 p$	19	$\Xi^0\Xi^0$
7	$\Sigma^+ p$	20	$\Lambda n / -\sqrt{\frac{1}{3}}\Sigma^0 n + \sqrt{\frac{2}{3}}\Sigma^- p$
8	$\Sigma^-\Sigma^-$	21	$\Lambda p / \sqrt{\frac{2}{3}}\Sigma^+ n + \sqrt{\frac{1}{3}}\Sigma^0 p$
9	$\frac{1}{\sqrt{2}}(\Sigma^-\Sigma^0 + \Sigma^0\Sigma^-)$	22	$\Lambda\Sigma^- / \Xi^- n$
10	$\frac{1}{\sqrt{6}}(\Sigma^-\Sigma^+ - 2\Sigma^0\Sigma^0 + \Sigma^+\Sigma^-)$	23	$\Lambda\Sigma^0 / \frac{1}{\sqrt{2}}(\Xi^- p - \Xi^0 n)$
11	$\frac{1}{\sqrt{2}}(\Sigma^0\Sigma^+ + \Sigma^+\Sigma^0)$	24	$\Lambda\Sigma^+ / \Xi^0 p$
12	$\Sigma^+\Sigma^+$	25	$\Lambda\Xi^- / \sqrt{\frac{1}{3}}\Sigma^0\Xi^- + \sqrt{\frac{2}{3}}\Sigma^-\Xi^0$
13	$\Sigma^-\Xi^-$	26	$\Lambda\Xi^0 / -\sqrt{\frac{2}{3}}\Sigma^+\Xi^- + \sqrt{\frac{1}{3}}\Sigma^0\Xi^0$
27	$\frac{1}{\sqrt{3}}(\Sigma^+\Sigma^- + \Sigma^0\Sigma^0 + \Sigma^-\Sigma^+) / \frac{1}{\sqrt{2}}(\Xi^0 n + \Xi^- p) / \Lambda\Lambda$		

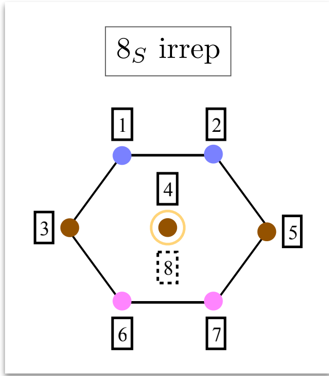

	Flavor channel
1	$\Lambda n / -\sqrt{\frac{1}{3}}\Sigma^0 n + \sqrt{\frac{2}{3}}\Sigma^- p$
2	$\Lambda p / \sqrt{\frac{2}{3}}\Sigma^+ n + \sqrt{\frac{1}{3}}\Sigma^0 p$
3	$\Lambda\Sigma^- / \Xi^- n$
4	$\Lambda\Sigma^0 / \frac{1}{\sqrt{2}}(\Xi^- p - \Xi^0 n)$
5	$\Lambda\Sigma^+ / \Xi^0 p$
6	$\Lambda\Xi^- / \sqrt{\frac{1}{3}}\Sigma^0\Xi^- + \sqrt{\frac{2}{3}}\Sigma^-\Xi^0$
7	$\Lambda\Xi^0 / -\sqrt{\frac{2}{3}}\Sigma^+\Xi^- + \sqrt{\frac{1}{3}}\Sigma^0\Xi^0$
8	$\frac{1}{\sqrt{3}}(\Sigma^+\Sigma^- + \Sigma^0\Sigma^0 + \Sigma^-\Sigma^+) / \frac{1}{\sqrt{2}}(\Xi^0 n + \Xi^- p) / \Lambda\Lambda$

J=0

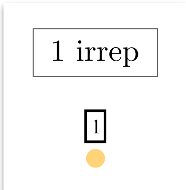

	Flavor channel
1	$\frac{1}{\sqrt{3}}(\Sigma^+\Sigma^- + \Sigma^0\Sigma^0 + \Sigma^-\Sigma^+) / \frac{1}{\sqrt{2}}(\Xi^0 n + \Xi^- p) / \Lambda\Lambda$

strangeness

I_3

M.L. Wagman et al (NPLQCD)
ARXIV:1706.06550

TWO-BARYON STATES AT THE SU(3) FLAVOR-SYMMETRIC POINT

SU(3) decomposition   Two-baryon states

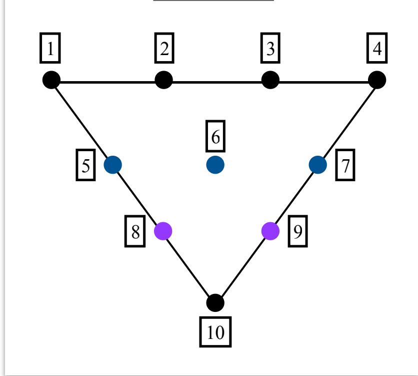

	Flavor channel
1	$\Sigma^- n$
2	$\sqrt{\frac{2}{3}}\Sigma^0 n+\sqrt{\frac{1}{3}}\Sigma^- p$
3	$-\sqrt{\frac{1}{3}}\Sigma^+ n+\sqrt{\frac{2}{3}}\Sigma^0 p$
4	$\Sigma^+ p$
5	$\frac{1}{\sqrt{2}}(\Sigma^-\Sigma^0-\Sigma^0\Sigma^-)/\Xi^- n/\Lambda\Sigma^-$
6	$\frac{1}{\sqrt{2}}(\Sigma^-\Sigma^+-\Sigma^+\Sigma^-)/\frac{1}{\sqrt{2}}(\Xi^- p-\Xi^0 n)/\Lambda\Sigma^0$
7	$\frac{1}{\sqrt{2}}(\Sigma^0\Sigma^+-\Sigma^+\Sigma^0)/\Xi^0 p/\Lambda\Sigma^+$
8	$\sqrt{\frac{1}{3}}\Sigma^0\Xi^-+\sqrt{\frac{2}{3}}\Sigma^-\Xi^0/\Lambda\Xi^-$
9	$-\sqrt{\frac{2}{3}}\Sigma^+\Xi^-+\sqrt{\frac{1}{3}}\Sigma^0\Xi^0/\Lambda\Xi^0$
10	$\frac{1}{\sqrt{2}}(\Xi^0\Xi^-$-$\Xi^-\Xi^0)$

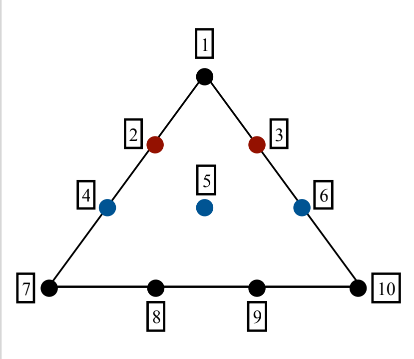

	Flavor channel
1	$\frac{1}{\sqrt{2}}(pn-np)$
2	$-\sqrt{\frac{1}{3}}\Sigma^0 n+\sqrt{\frac{2}{3}}\Sigma^- p/\Lambda n$
3	$\sqrt{\frac{2}{3}}\Sigma^+ n+\sqrt{\frac{1}{3}}\Sigma^0 p/\Lambda p$
4	$\frac{1}{\sqrt{2}}(\Sigma^-\Sigma^0-\Sigma^0\Sigma^-)/\Xi^- n/\Lambda\Sigma^-$
5	$\frac{1}{\sqrt{2}}(\Sigma^-\Sigma^+-\Sigma^+\Sigma^-)/\frac{1}{\sqrt{2}}(\Xi^- p-\Xi^0 n)/\Lambda\Sigma^0$
6	$\frac{1}{\sqrt{2}}(\Sigma^0\Sigma^+-\Sigma^+\Sigma^0)/\Xi^0 p/\Lambda\Sigma^+$
7	$\Sigma^-\Xi^-$
8	$-\sqrt{\frac{2}{3}}\Sigma^0\Xi^-+\sqrt{\frac{1}{3}}\Sigma^-\Xi^0$
9	$\sqrt{\frac{1}{3}}\Sigma^+\Xi^-+\sqrt{\frac{2}{3}}\Sigma^0\Xi^0$
10	$\Sigma^+\Xi^0$

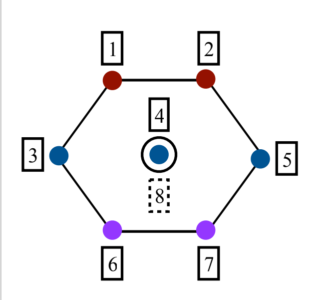

	Flavor channel
1	$-\sqrt{\frac{1}{3}}\Sigma^0 n+\sqrt{\frac{2}{3}}\Sigma^- p/\Lambda n$
2	$\sqrt{\frac{2}{3}}\Sigma^+ n+\sqrt{\frac{1}{3}}\Sigma^0 p/\Lambda p$
3	$\frac{1}{\sqrt{2}}(\Sigma^-\Sigma^0-\Sigma^0\Sigma^-)/\Xi^- n/\Lambda\Sigma^-$
4	$\frac{1}{\sqrt{2}}(\Sigma^-\Sigma^+-\Sigma^+\Sigma^-)/\frac{1}{\sqrt{2}}(\Xi^- p-\Xi^0 n)/\Lambda\Sigma^0$
5	$\frac{1}{\sqrt{2}}(\Sigma^0\Sigma^+-\Sigma^+\Sigma^0)/\Xi^0 p/\Lambda\Sigma^+$
6	$\sqrt{\frac{1}{3}}\Sigma^0\Xi^-+\sqrt{\frac{2}{3}}\Sigma^-\Xi^0/\Lambda\Xi^-$
7	$-\sqrt{\frac{2}{3}}\Sigma^+\Xi^-+\sqrt{\frac{1}{3}}\Sigma^0\Xi^0/\Lambda\Xi^0$
8	$\frac{1}{\sqrt{2}}(\Xi^0 n+\Xi^- p)$

J=1

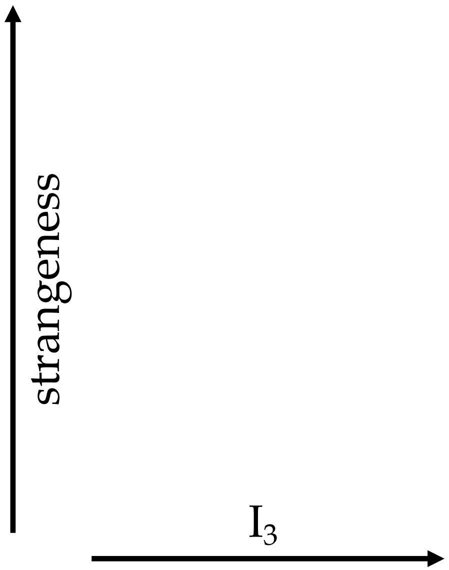

M.L. Wagman et al (NPLQCD)
ARXIV:1706.06550

TWO-BARYON STATES AT THE SU(3) FLAVOR-SYMMETRIC POINT

LQCD → FEW-BODY CALCS → NUCLEAR MANY-BODY CALCS

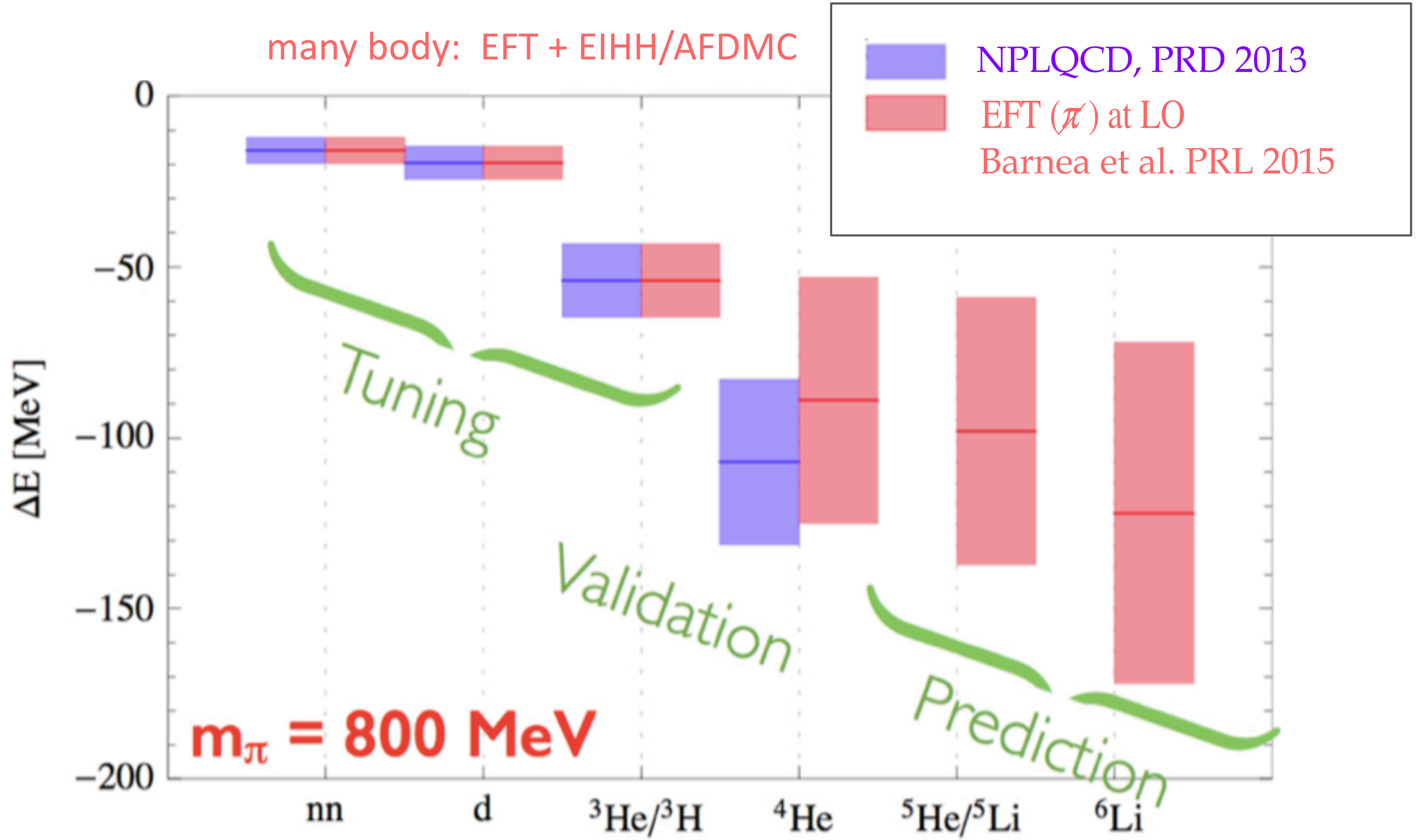

N. Barnea, L. Contessi, D. Gazit, F. Pederiva, and U. van Kolck, PRL **114** (2015) 052501

L. Contessi, A. Lovato, F. Pederiva, A. Roggero, J. Kirscher and U. van Kolck, PLB **772** (2017) 839
Ground-state properties of ^{4}He and ^{16}O extrapolated from lattice QCD with pionless EFT

LQCD – QMC symbiosis

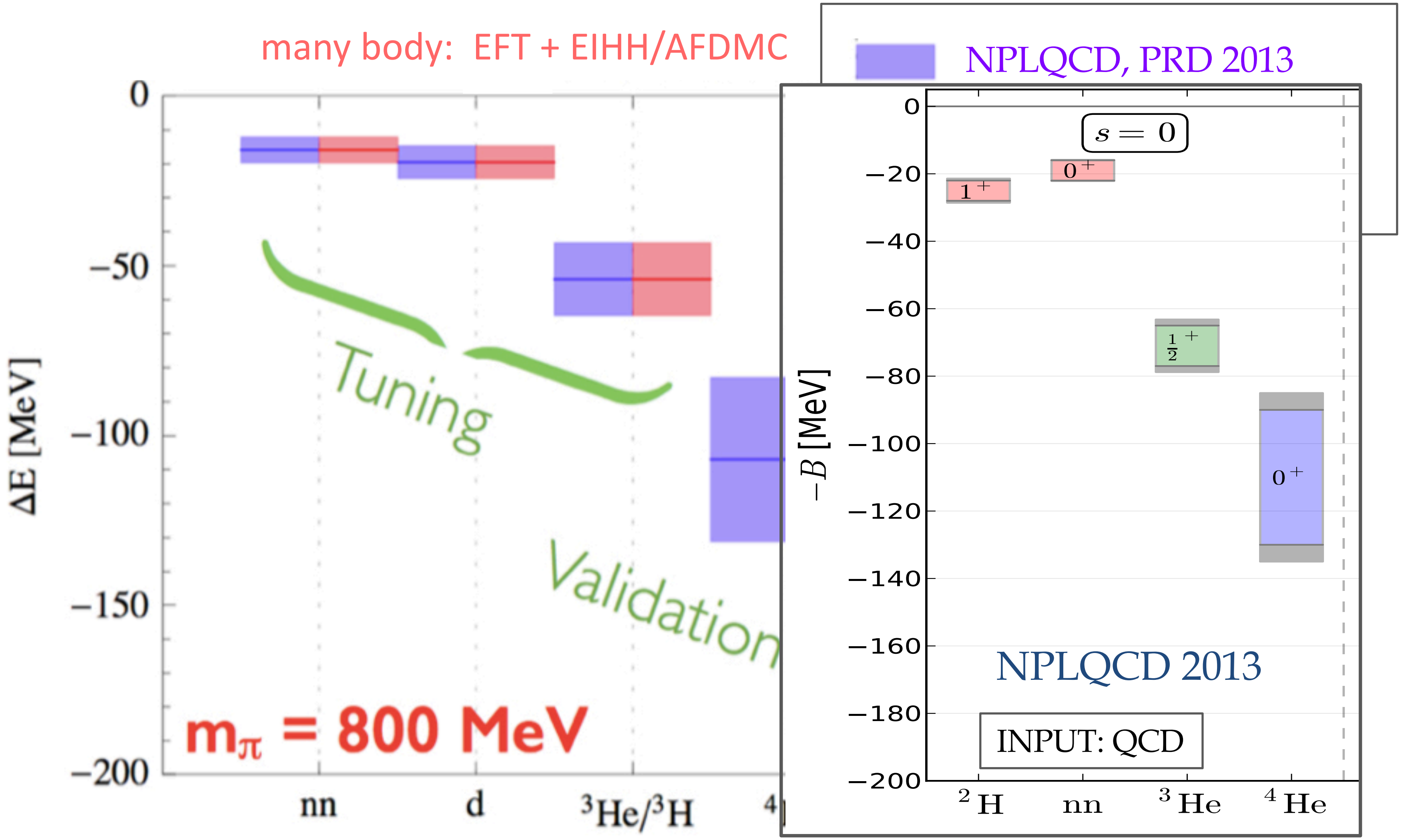

L. Contessi, A. Lovato, F. Pederiva, A. Roggero, J. Kirscher and U. van Kolck, PLB **772** (2017) 839
Ground-state properties of ^{4}He and ^{16}O extrapolated from lattice QCD with pionless EFT

For numerical calculations in QCD, the theory is formulated on a (Euclidean) space-time lattice

((anti) periodic (time) spatial boundary conditions) $N_s \times N_s \times N_s \times N_t$

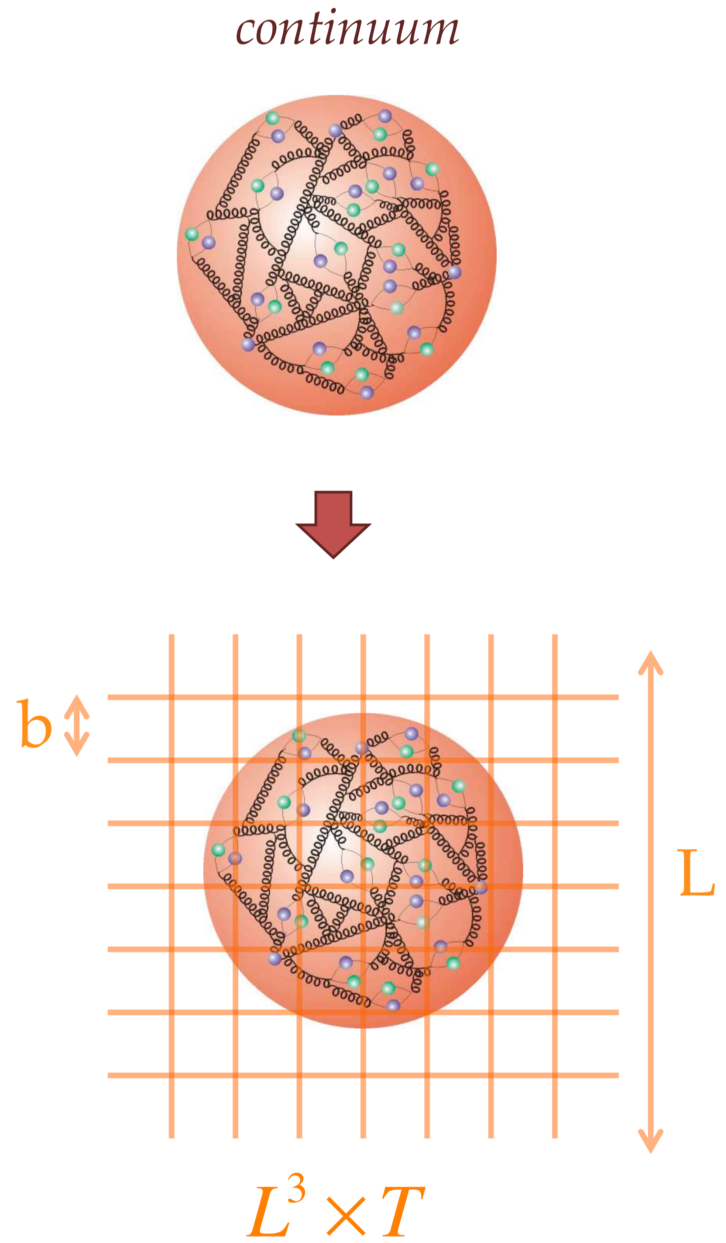

LQCD is a non-perturbative implementation of Field Theory, which uses the Feynman path-integral approach to evaluate transition matrix elements

Wilson, 1970
Monte-Carlo (probabilistic) evaluation of the Euclidean space path integral

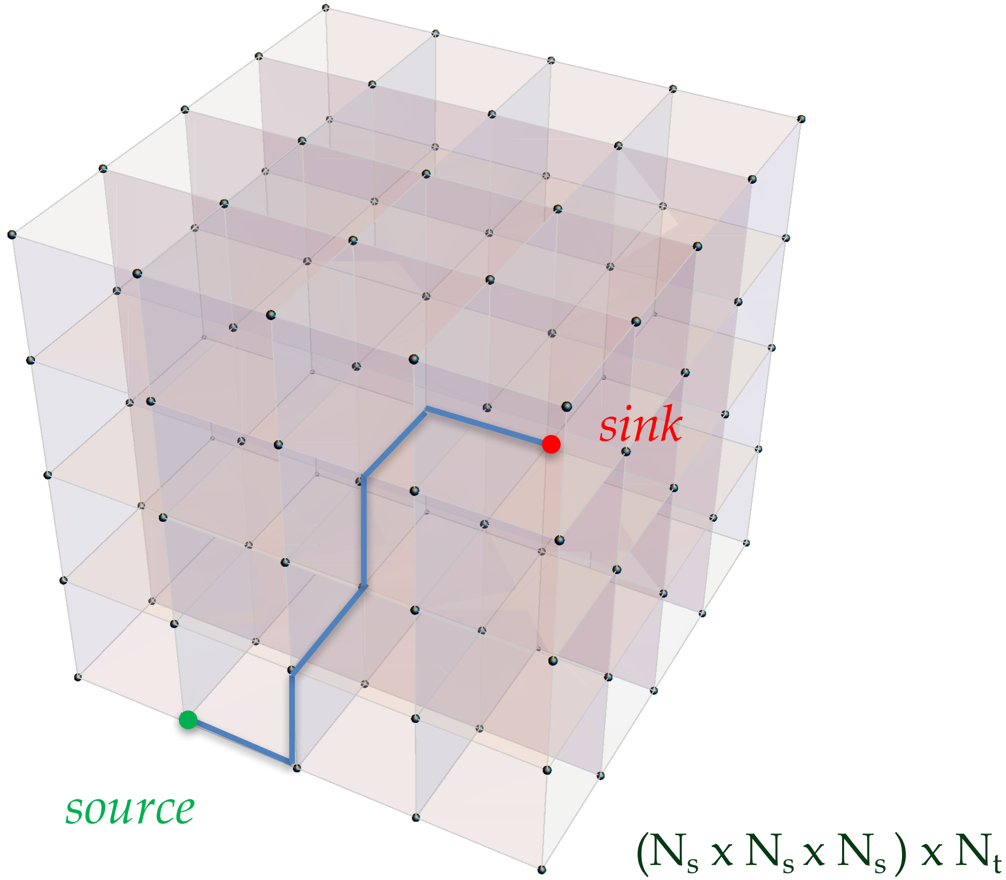

(anti) periodic (time) spatial boundary conditions

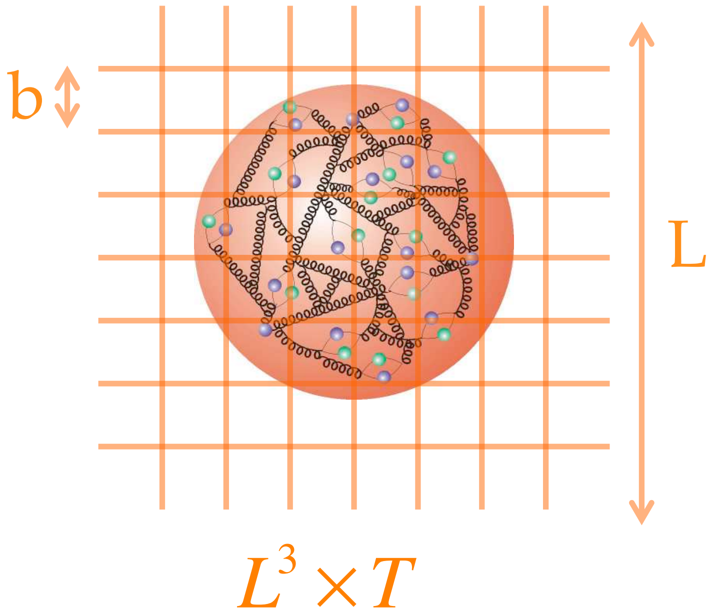

$$L >> \text{ relevant scales } >> b \quad \left(\frac{1}{L} << m_\pi << \Lambda_\chi << \frac{1}{b} \right)$$

→ *i.e.* finite number of d.o.f. (finite volume)

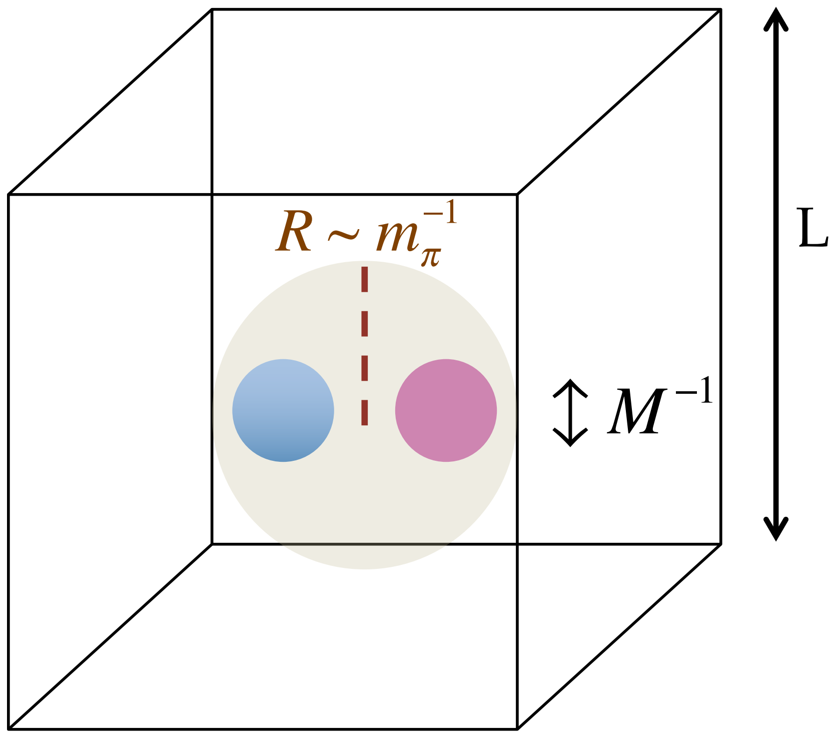

Lüscher, 1990

$R < \frac{L}{2}$

nucleon-nucleon scattering

$\Rightarrow m_\pi L >> 1$ (infrared cutoff)

$b << \frac{1}{M_N}$ (ultraviolet cutoff)

$L >>$ relevant scales $>> b$ $\left(\frac{1}{L} << m_\pi << \Lambda_\chi << \frac{1}{b} \right)$

→ *i.e.* finite number of d.o.f. (finite volume)

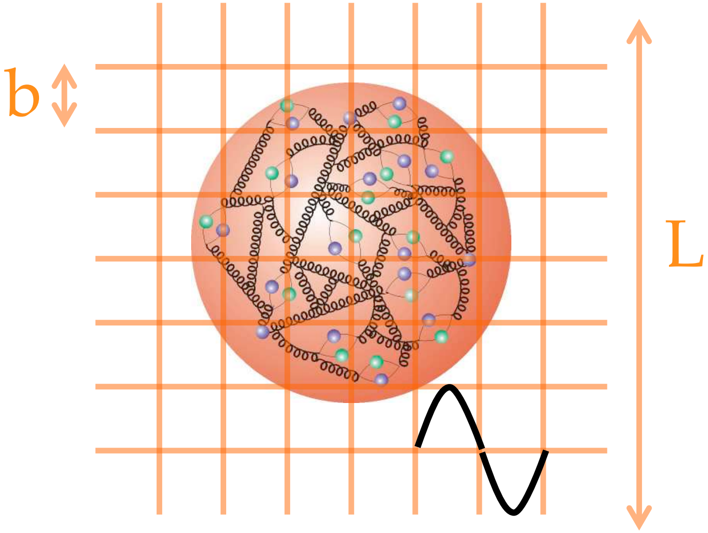

$x = b\,(n_1, n_2, n_3, n_4) \qquad n_j \in \mathbb{Z}$

$L^3 \times T$

$\lambda_{\min} = 2b$ shortest wave length

$$\left.\begin{array}{c} \vec{p} = \frac{2\pi}{L}\vec{n}, \quad n_\mu \in \mathbb{Z} \\ x_\mu = m_\mu b, \quad \text{with } m_\mu = 0,1,2,\ldots N-1, \quad \text{and } L = Nb \end{array}\right\} \Rightarrow p_{\max} = n_{\max}\frac{2\pi}{L} = \frac{N}{2}\frac{2\pi}{Nb} = \frac{\pi}{b}$$

cut-off

(larger wave vector)

Computational cost increases as light quark masses decrease:
work with unphysical values of the quark masses and perform the correspondig extrapolation

Direct Lattice QCD extraction ⟷ Compute correlation functions

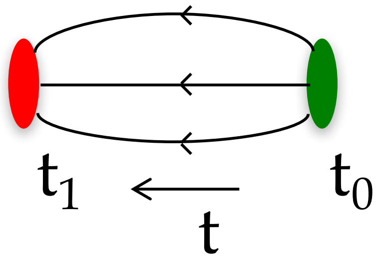

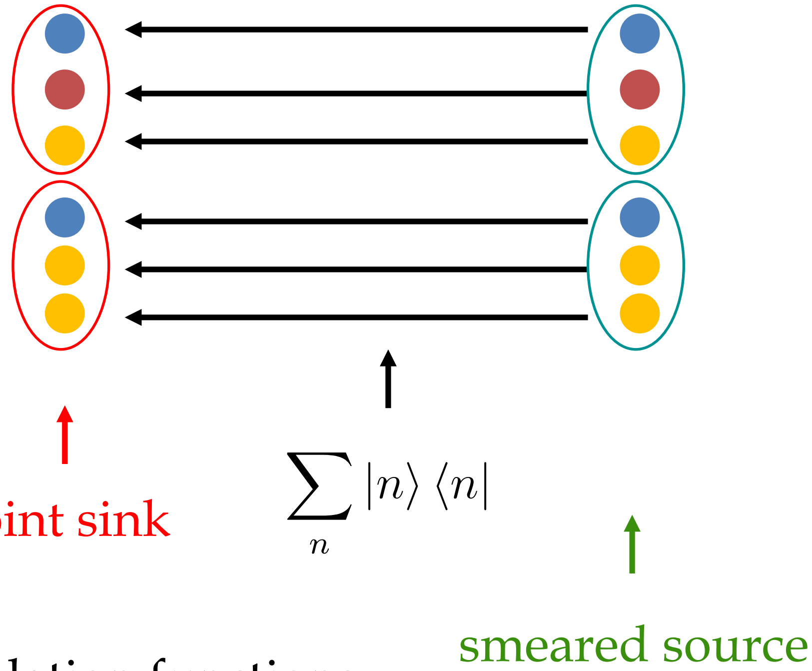

construction of SS/SP correlation functions

$$C_{\hat{O},\hat{O}'}(t,\vec{d}) = \sum_{\vec{x}} e^{2\pi i \vec{d}\vec{x}/L} \langle 0|\hat{O}'(\vec{x},t)\hat{O}^{\dagger}(\vec{0},0)|0\rangle$$

$$= \underbrace{Z_0^{snk} Z_0^{\dagger src} e^{-E^{(0)}t}}_{\text{dominates at large t}} + Z_1^{snk} Z_1^{\dagger src} e^{-E^{(1)}t} + \cdots$$

projected into total momentum $\frac{2\pi\vec{d}}{L}$

Determination of the energy levels:

- Use a linear combination of SS/SP correlation functions to remove the excited-state contamination of the lowest lying state at earlier times
  (Matrix-Prony method/GPoF method)

- Perform a correlated χ^2 fit to single or two-exponential forms

- Work with an effective mass(energy) function:

$$C_{\hat{O},\hat{O}'}(\tau;\ \vec{d},\tau_J) = \frac{1}{\tau_J}\log\left[\frac{C_{\hat{O},\hat{O}'}(\tau;\vec{d})}{C_{\hat{O},\hat{O}'}(\tau+\tau_J;\vec{d}\,)}\right] \rightarrow\ E_0 \qquad \text{at large times}$$

$32^3\times 48$ $\quad m_\pi \sim 806$ MeV

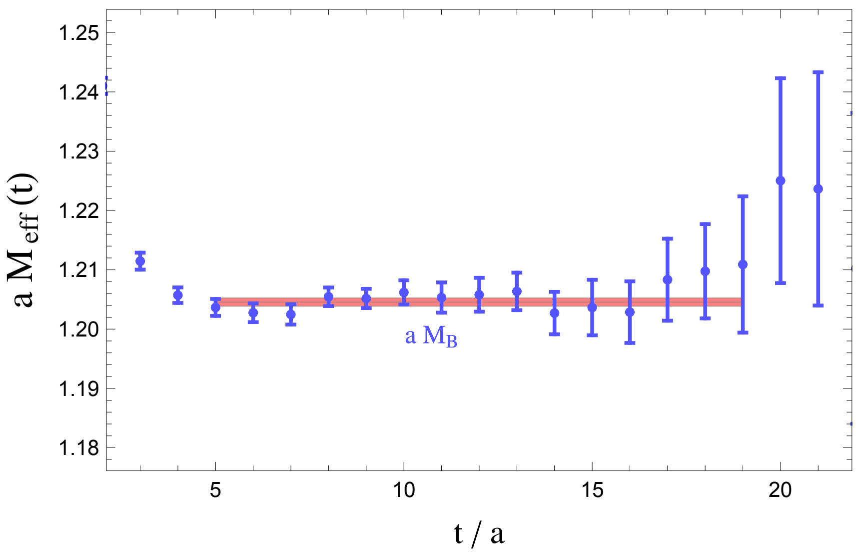

$32^3\times 96$ $\quad m_\pi \sim 450$ MeV

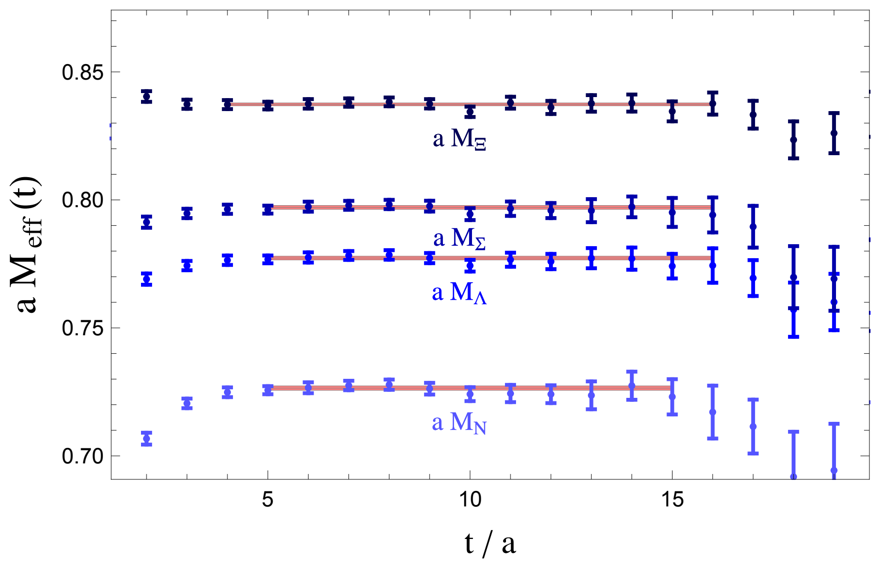

A. Parreño et al (NPLQCD), PRD 95 (2017), 114513

Determination of the energy levels:

- Use a linear combination of SS/SP correlation functions to remove the excited-state contamination of the lowest lying state at earlier times
  (Matrix-Prony method/GPoF method)

- Perform a correlated χ^2 fit to single or two-exponential forms

- Work with an effective mass(energy) function:

$$C_{\hat{O},\hat{O}'}(\tau;\ \vec{d},\tau_J) = \frac{1}{\tau_J}\log\left[\frac{C_{\hat{O},\hat{O}'}(\tau;\vec{d})}{C_{\hat{O},\hat{O}'}(\tau+\tau_J;\vec{d})}\right] \rightarrow\ E_0 \qquad \text{at large times}$$

Using the single and two-body correlation functions, one can compute the shift in the energy of the system resulting from two-body interactions:

$$R(\tau;\mathbf{d}) \ = \ \frac{C_{\hat{\mathcal{O}}_{BB},\hat{\mathcal{O}}'_{BB}}(\tau;\mathbf{d})}{\left[C_{\hat{\mathcal{O}}_{B},\hat{\mathcal{O}}'_{B}}(\tau;\mathbf{0})\right]^2} = \mathcal{A}_1 e^{-(E_{BB}^{(0)}-2M_B)\tau} \times \frac{1+\mathcal{A}_2 e^{-(E_{BB}^{(1)}-E_{BB}^{(0)})\tau}+\ldots}{\left[1+\mathcal{A}_3 e^{-(E_{B}^{(1)}-M_B)\tau}+\ldots\right]^2}$$

$$R^{\text{eff}}(\tau;\ \vec{d},\tau_J) = \frac{1}{\tau_J}\log\left[\frac{R(\tau;\vec{d})}{R(\tau+\tau_J;\vec{d})}\right] \rightarrow\ \overline{\Delta E} \qquad \text{at large times}$$

$m_\pi \sim 806$ MeV

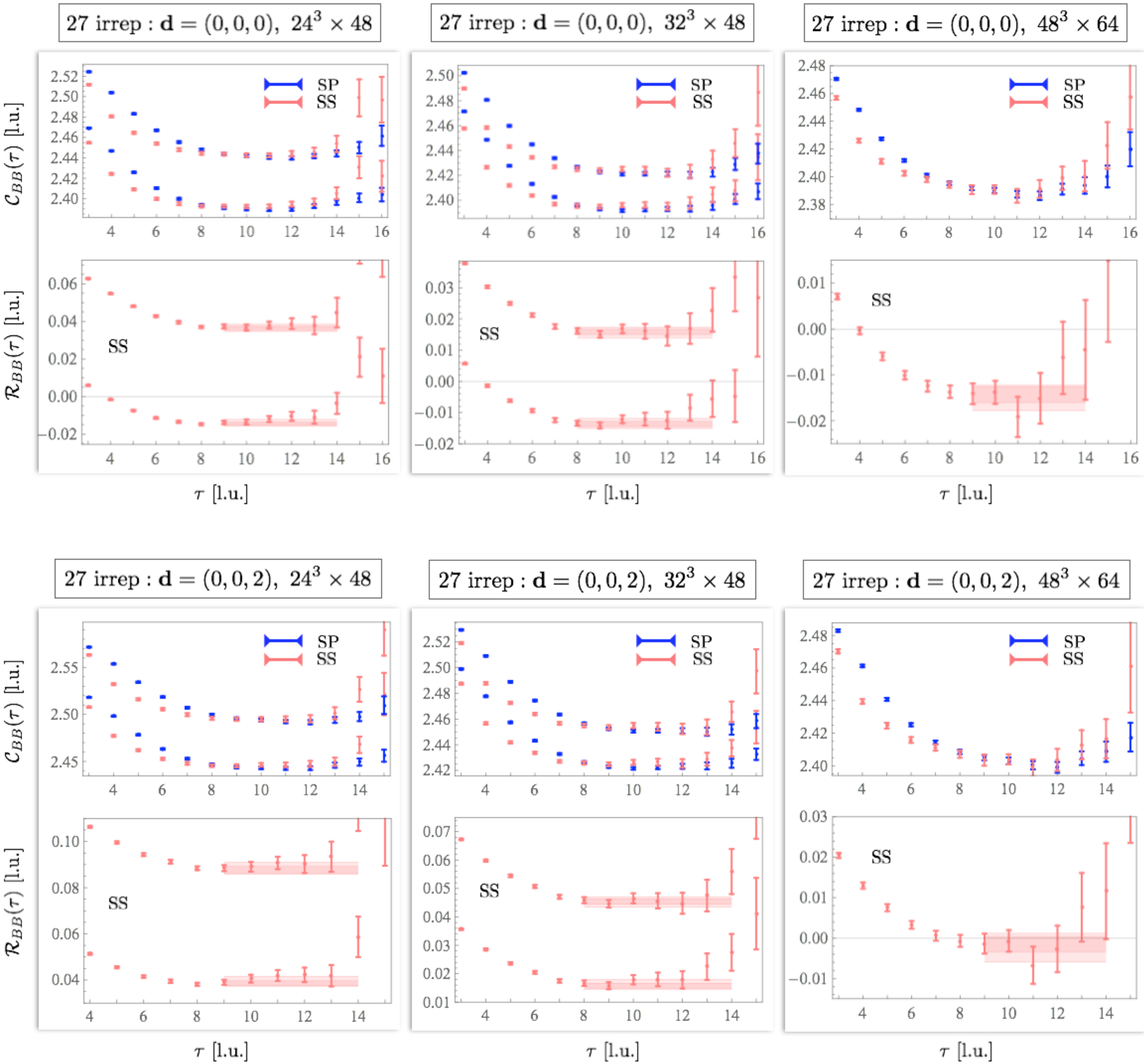

J=0

(nn)

M.L. Wagman et al (NPLQCD)
PRD, ARXIV:1706.06550

Energy shifts

$$\overline{\Delta E} = E_{BB'} - 2M_B$$

10 kinematical points for each irrep

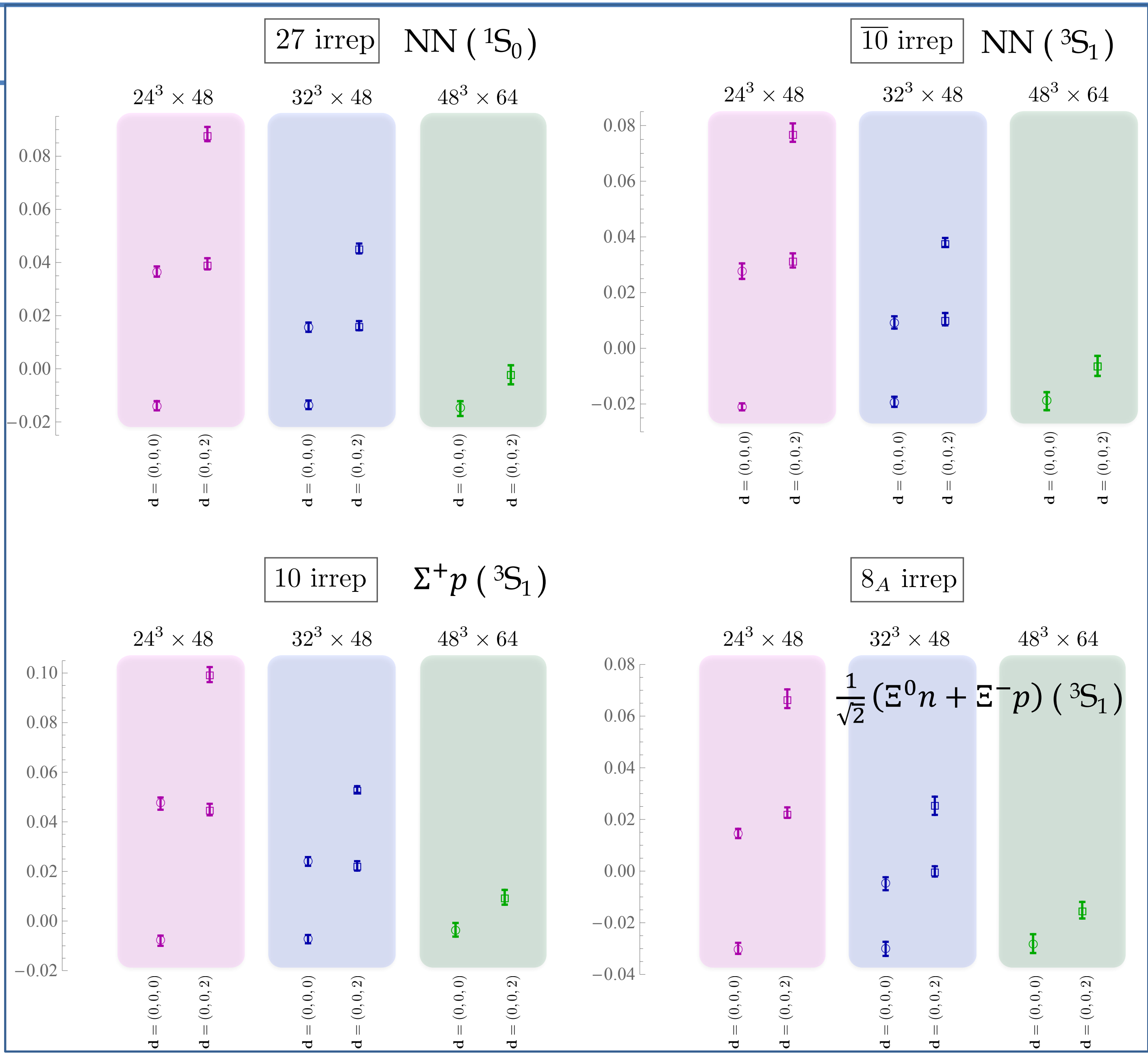

M.L. Wagman et al (NPLQCD), PRD, ARXIV:1706.06550

$m_\pi \sim 806$ MeV

Energy shifts – Location of bound states

$\overline{\Delta E} = E_{BB'} - 2M_B$

10 kinematical points for each irrep

input to constrain

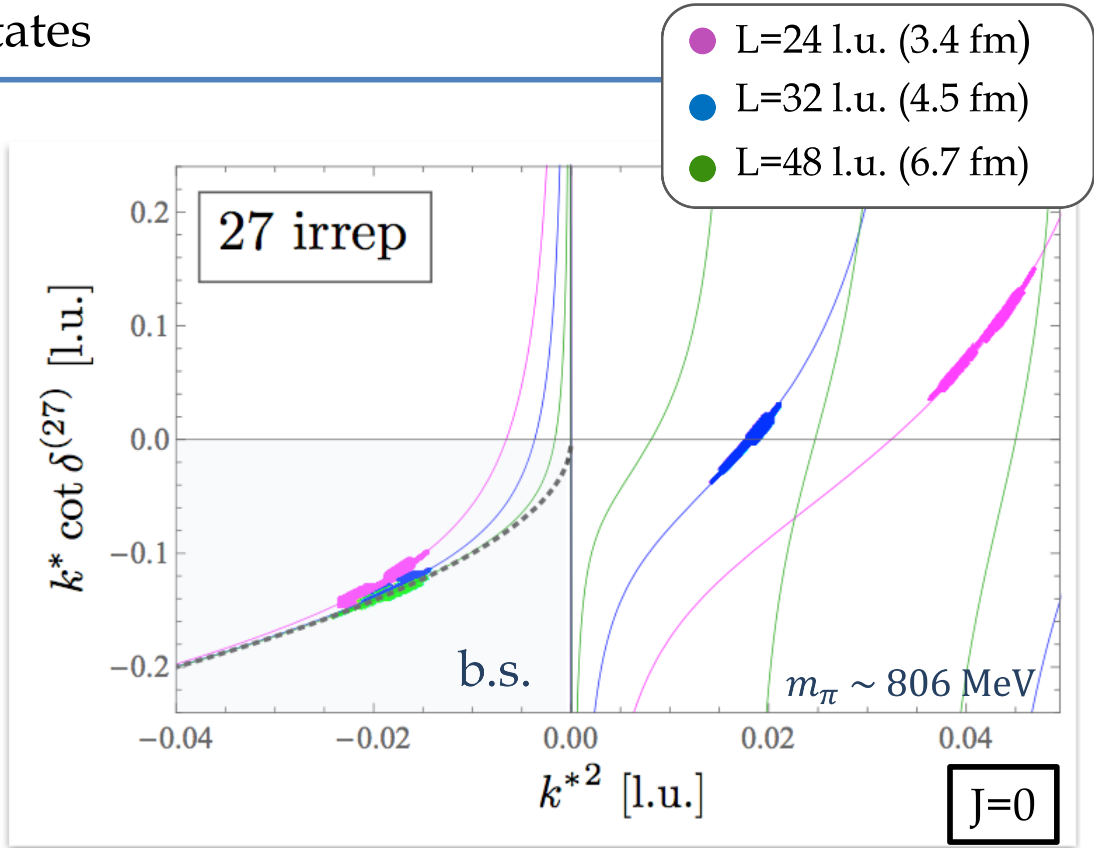

L=24 l.u. (3.4 fm)
L=32 l.u. (4.5 fm)
L=48 l.u. (6.7 fm)

$$k \cot\delta(k) = \frac{1}{\pi L} \sum_{\vec{n}} \frac{1}{\vec{n}^2 - q^2} \qquad \vec{n} \in Z^3 \qquad q = \frac{Lk}{2\pi}$$

$$\mathcal{A} \sim \frac{4\pi}{M} \frac{1}{p\cot\delta(p) - ip}$$

infinite volume

b.s. $p^2 = -\gamma^2$

$\cot\delta(i\gamma) = i$

finite volume:

$$\cot\delta(i\gamma)\Big|_{k=i\gamma} = i - i\sum_{\vec{m}\neq\vec{0}} \frac{e^{-|\vec{m}|\gamma L}}{|\vec{m}|\gamma L}$$

$$k^* \cot\delta(k^*) = -\sqrt{-k^{*2}} \quad \text{............}$$

Binding energies

$$\overline{\Delta E} = E_{BB'} - 2M_B$$

10 kinematical points for each irrep

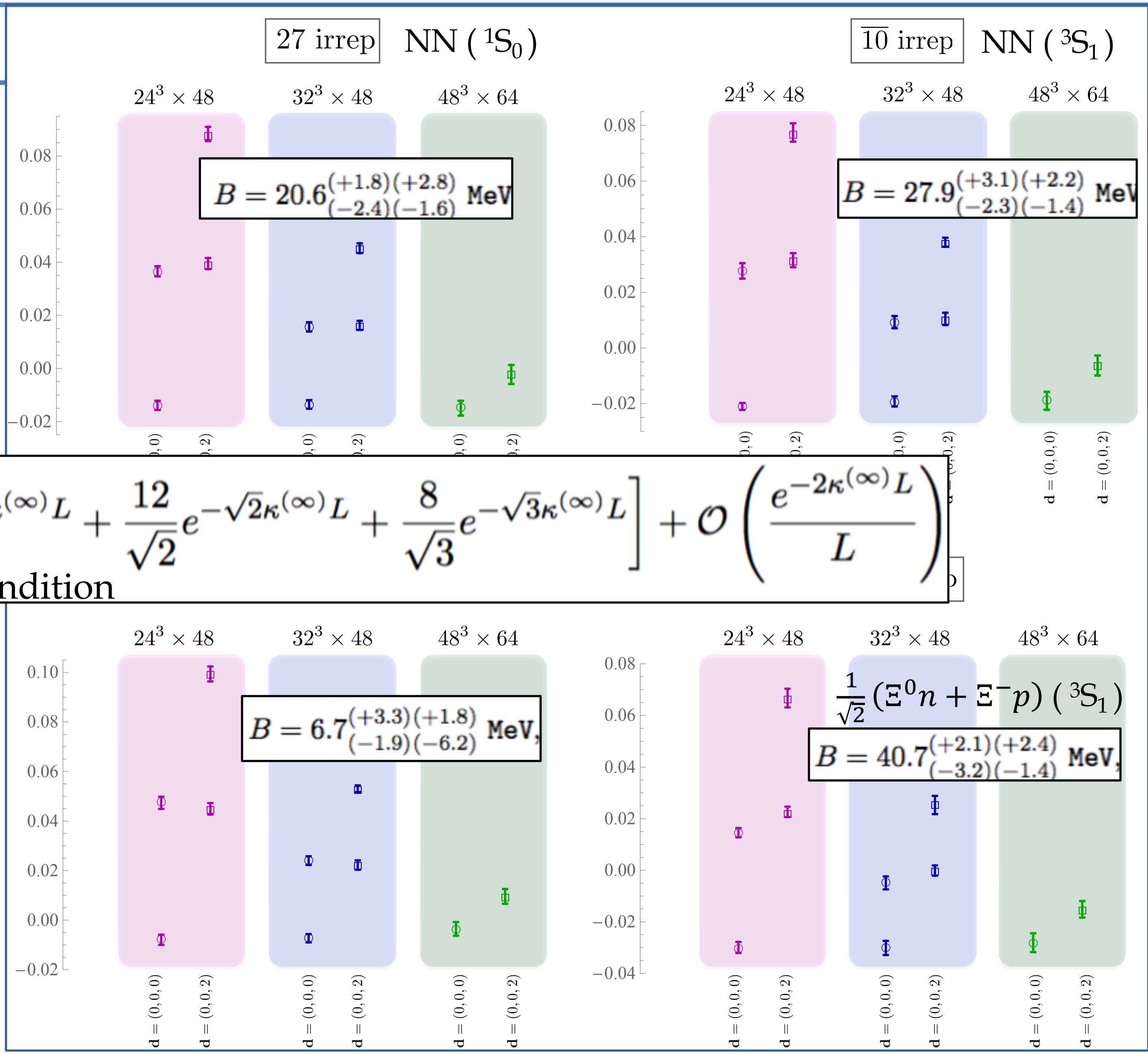

$$|k^*| = \kappa^{(\infty)} + \frac{Z^2}{L}\left[6e^{-\kappa^{(\infty)}L} + \frac{12}{\sqrt{2}}e^{-\sqrt{2}\kappa^{(\infty)}L} + \frac{8}{\sqrt{3}}e^{-\sqrt{3}\kappa^{(\infty)}L}\right] + \mathcal{O}\left(\frac{e^{-2\kappa^{(\infty)}L}}{L}\right)$$

Lüscher's quantization condition

$$B = -2\sqrt{-\kappa^{(\infty)2} + M_B^2} + 2M_B$$

M.L. Wagman et al (NPLQCD), PRD, ARXIV:1706.06550

$m_\pi \sim 806$ MeV

Energy shifts – Location of bound states – Effective Range Expansion

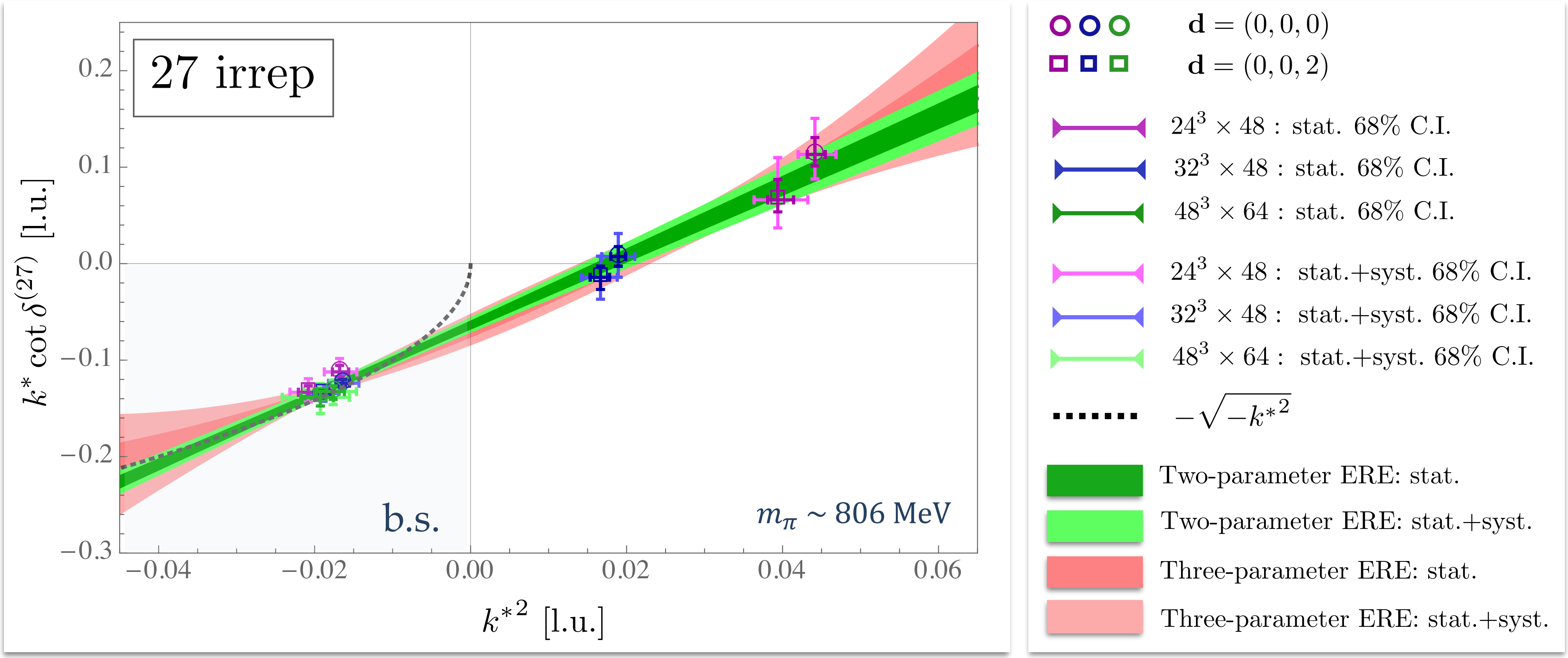

ERE $k^* \cot\delta(k^*) = -\frac{1}{a} + \frac{1}{2} r k^{*2} + P k^{*4} + \cdots$

M.L. Wagman et al (NPLQCD) PRD, ARXIV:1706.06550

Energy shifts – Location of bound states – Effective Range Expansion

M.L. Wagman et al (NPLQCD) PRD, ARXIV:1706.06550

$m_\pi \sim 806$ MeV

$$a^{-1} = 0.44^{(+4)(+8)}_{(-5)(-8)}\ \mathrm{fm}^{-1}$$

$$r = 1.04^{(+10)(+18)}_{(-10)(-18)}\ \mathrm{fm}$$

$$a^{-1} = 0.63^{(+6)(+10)}_{(-5)(-11)}\ \mathrm{fm}^{-1}$$

$$r = 0.70^{(+16)(+12)}_{(-2)(-20)}\ \mathrm{fm}$$

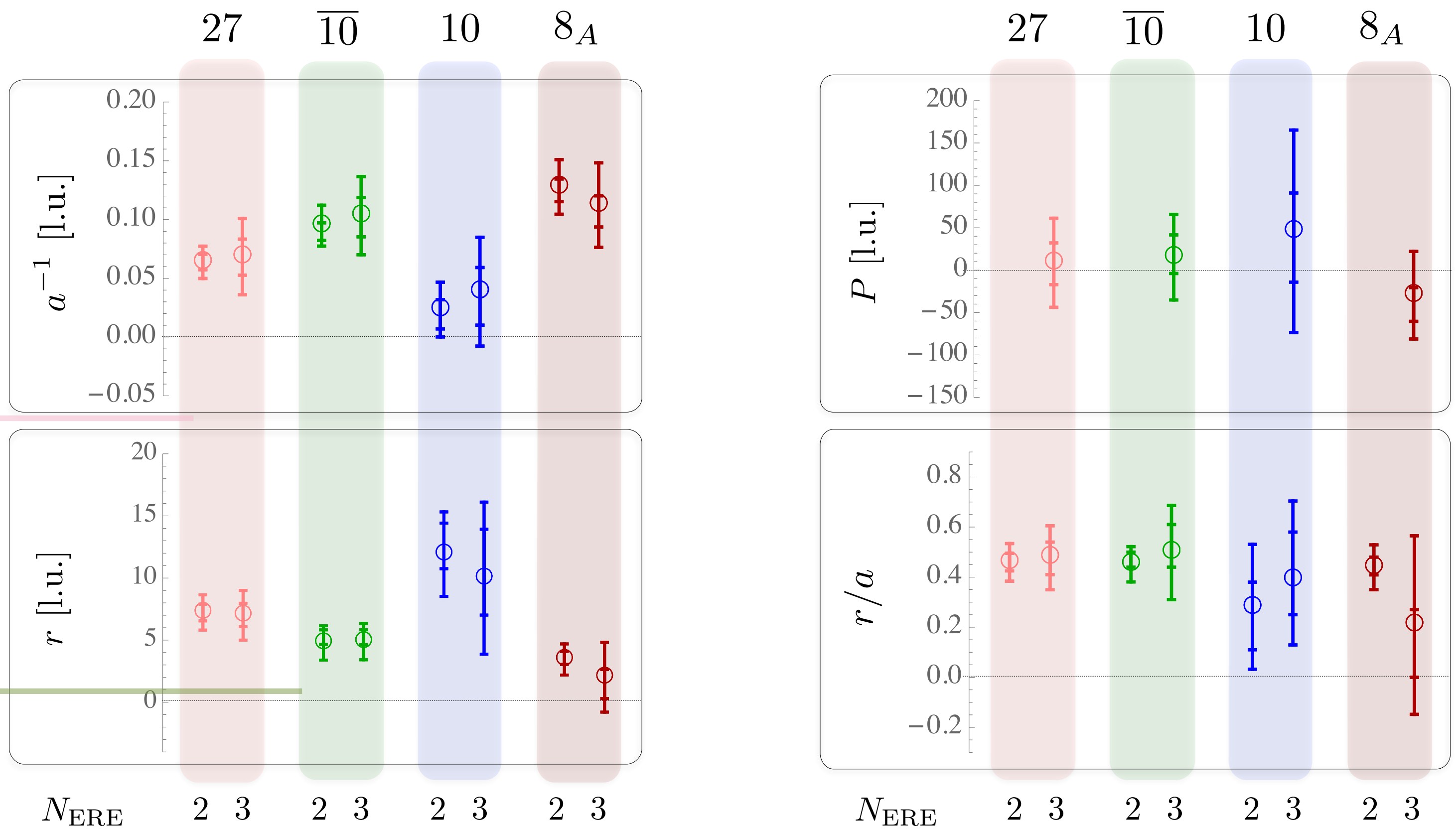

Energy shifts – Location of bound states – Effective Range Expansion

M.L. Wagman et al (NPLQCD) PRD, ARXIV:1706.06550

$m_\pi \sim 806$ MeV

$$a^{-1} = 0.44^{(+4)(+8)}_{(-5)(-8)}\ \text{fm}^{-1}$$

$$r = 1.04^{(+10)(+18)}_{(-10)(-18)}\ \text{fm}$$

$$a^{-1} = 0.63^{(+6)(+10)}_{(-5)(-11)}\ \text{fm}^{-1}$$

$$r = 0.70^{(+16)(+12)}_{(-2)(-20)}\ \text{fm}$$

K. Orginos et al (NPLQCD) PRD92,114512 (2015)

$m_\pi \sim 450$ MeV

$$a^{-1}(\,^1S_0) = 0.05^{(+0.06)(+0.08)}_{(-0.08)(-0.14)}\ \text{fm}^{-1}$$

$$r\,(\,^1S_0) = 2.96^{(+43)(+87)}_{(-34)(-055)}\ \text{fm}$$

$$a^{-1}(\,^3S_1) = -0.09^{(+0.15)(+0.19)}_{(-0.23)(-0.39)}\ \text{fm}^{-1}$$

$$r\,(\,^3S_1) = 3.4^{(+1.0)(+1.5)}_{(-0.7)(-0.8)}\ \text{fm}$$

Nature

m_π physical

$$a^{-1}(\,^1S_0) \approx -0.05\quad \text{fm}^{-1}$$

$$r\,(\,^1S_0) \approx 2.75\ \text{fm}$$

$$a^{-1}(\,^3S_1) \approx 0.18\ \text{fm}^{-1}$$

$$r\,(\,^3S_1) \approx 1.75\ \text{fm}$$

NPLQCD, Phys. Rev .Lett. 113 (2014) 25, 252001x

NPLQCD

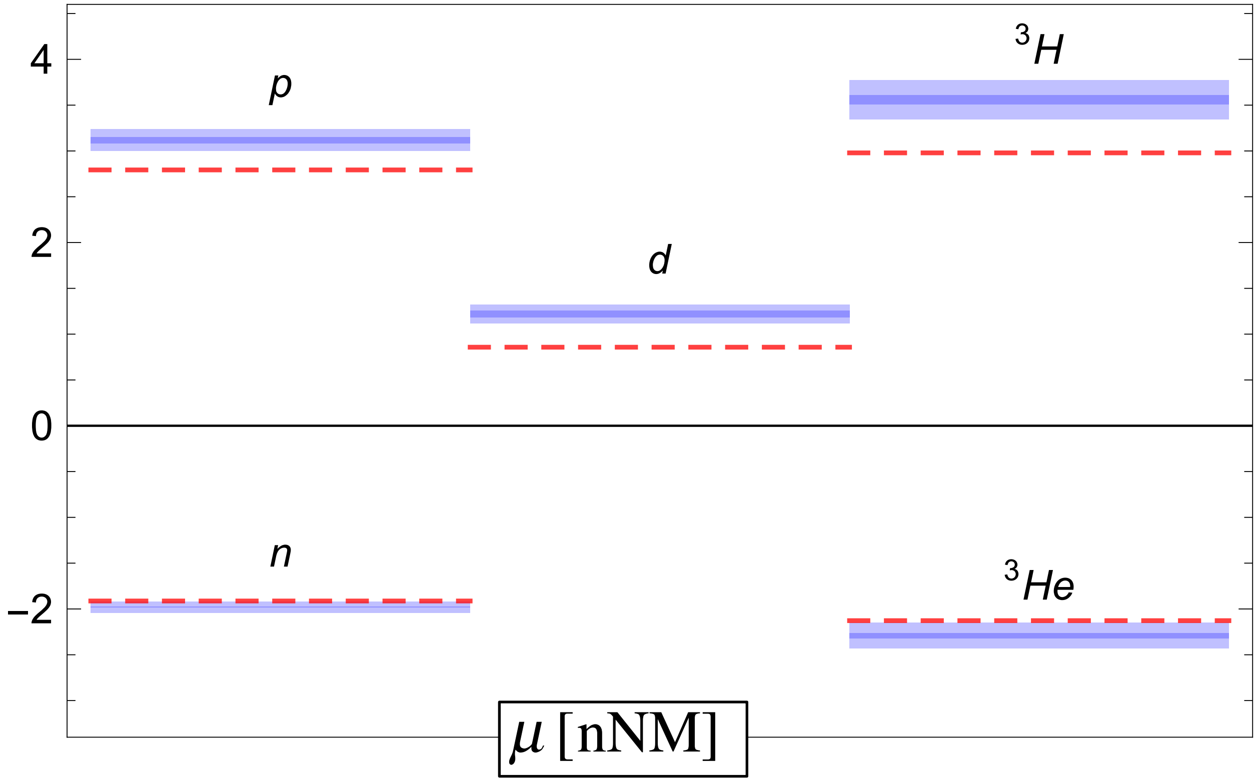

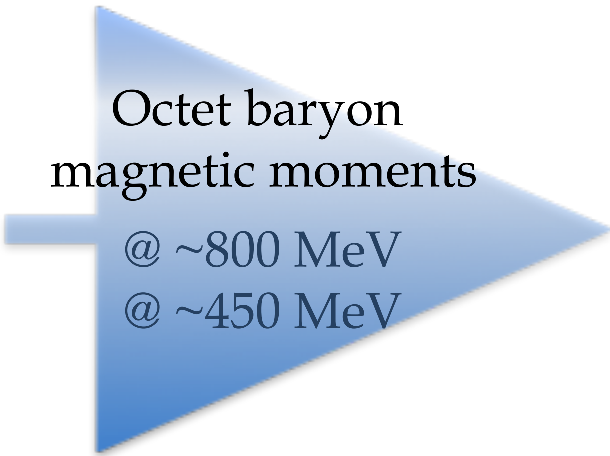

$$\text{nNM} = \frac{e}{2M_N^{\text{latt}}} = \frac{e}{2M_N(m_\pi^{\text{latt}})}$$

Shell-model predictions

$$\mu(^3H) = \mu_p$$

$$\mu(^3He) = \mu_n$$

$$\mu_d = \mu_n + \mu_p$$

LQCD @ $m_\pi \sim 800$ MeV

experiment

LQCD calculations of magnetic moments

NPLQCD, PRD95, 114513 (2017)

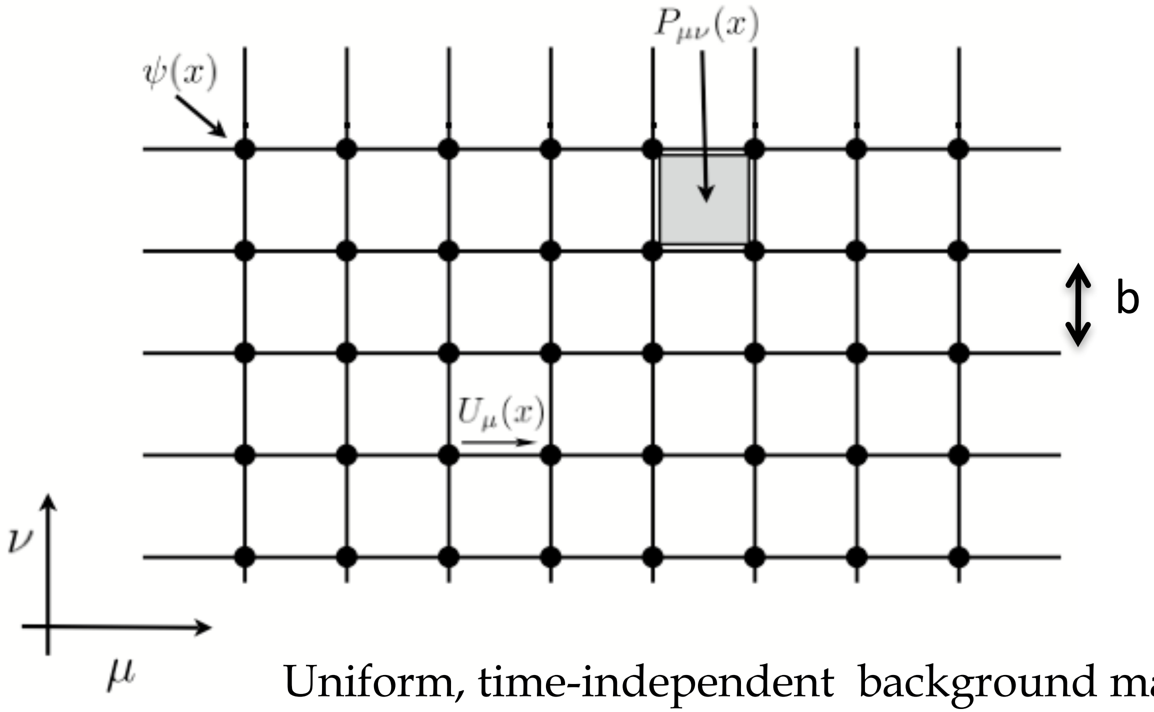

$$U_\mu^b(x) \equiv e^{ig\int_x^{x+b\mu} A_\mu dx^\mu} = e^{igbA_\mu^b(x)}$$

($SU(3)_c$ matrices, "links")

$$U_\mu(x+L\hat{\nu}) = U_\mu(x)$$

Uniform, time-independent background magnetic field $\vec{B} = \hat{z} \cdot B$

$$U_\mu^b(x) \to U_\mu^b(x) U_\mu^{\text{ext}}(x)$$

$$U_0^{\text{ext}}(x) = U_3^{\text{ext}}(x) = 1$$

$$U_1^{\text{ext}}(x) = \begin{cases} 1 & for\ x_1 \neq L-b \\ \exp\left(-i\, Q\, n\, \frac{2\pi x_2}{L}\right) & for x_1 = L-b \end{cases}$$

$$U_2^{\text{ext}}(x) = \exp\left(i\, Q\, n\, \frac{2\pi b x_1}{L^2}\right)$$

G. t'Hooft, 1979

U(1) flux through each plaquette = $e^{iQeF_{\mu\nu}}$,
with $F_{12} = -F_{21} = B_z$

$$\boxed{QeB_z = \frac{2\pi}{L^2} n}$$

$n = 3, -6, 12$

LQCD calculations of magnetic moments

NPLQCD, PRD95, 114513 (2017)

valence quarks   sea quarks

$$\langle O(U,q,\bar{q})\rangle = \frac{1}{Z}\int [dU] \prod_f \underbrace{\left(D[U]+m_f\right)^{-1}}_{\text{propagators}} \underbrace{\det\left(D[U]+m_f\right)\ e^{-S_g[U]}}_{\text{configurations}\ (\sim P(U))}$$

background electromagnetic field couples also to sea-quark degrees of freedom through the fermionic determinant.

$SU(3)_f$ sea quark contributions ~ Q_u + Q_d + Q_s

$$U_\mu^b(x) \rightarrow U_\mu^b(x) U_\mu^{\text{ext}}(x)$$

$$U_0^{\text{ext}}(x) = U_3^{\text{ext}}(x) = 1$$

$$U_1^{\text{ext}}(x) = \begin{cases} 1 & for\ x_1 \neq L-b \\ \exp\left(-i\,Q\,n\,\frac{2\pi x_2}{L}\right) & for\ x_1 = L-b \end{cases}$$

$$U_2^{\text{ext}}(x) = \exp\left(i\,Q\,n\,\frac{2\pi b x_1}{L^2}\right)$$

G. t'Hooft, 1979

U(1) flux through each plaquette = $e^{iQeF_{\mu\nu}}$, with $F_{12} = -F_{21} = B_z$

$$QeB_z = \frac{2\pi}{L^2} n$$

$n = 3, -6, 12$

LQCD calculations of magnetic moments

NPLQCD, PRD95, 114513 (2017)

$$E_B^{(s)}(B_z) = M_B + \frac{|Q_B e B_z|}{M_B}\left(n_L + \frac{1}{2}\right) - 2\,\mu_B s\, B_z - 2\pi\, \beta_B^{(M0)}|B|^2 - 2\pi\, \beta_B^{(M2)}\langle \hat{T}_{ij} B_i B_j \rangle \quad + \cdots$$

$$\left(s = \pm\frac{1}{2}, p_z = 0\right)$$

n_L Landau level
occupied by the baryon
(charged particles)

$O(B^2)$ (polarizabilities)

$$\delta E \equiv E_B^{(+1/2)}(\vec{B}) - E_B^{(-1/2)}(\vec{B}) = -2\,\mu_B\, B_z + \cdots$$

Determination of the magnetic moments relies on the determination of the Zeeman splittings

$$R_i(t) = \frac{G_i^{(+\frac{1}{2})}(t, n_\Phi)}{G_i^{(-\frac{1}{2})}(t, n_\Phi)} \Big/ \frac{G_i^{(+\frac{1}{2})}(t, 0)}{G_i^{(-\frac{1}{2})}(t, 0)}$$

$$\frac{1}{R_i(t)} \xrightarrow{t\to\infty} Z e^{-\delta E^B t}$$

$$QeB_z = \frac{2\pi}{L^2} n$$

$n = 3, -6, 12$

LQCD calculations of magnetic moments

NPLQCD, PRD95, 114513 (2017)

	L/a	T/a	β	am_l	am_s	a[fm]	m_π[MeV]	$N_{\rm cfg}$
I	32	48	6.1	−0.2450	−0.2450	0.1453(16)	806.9(8.9)	1006

$SU(3)_f$

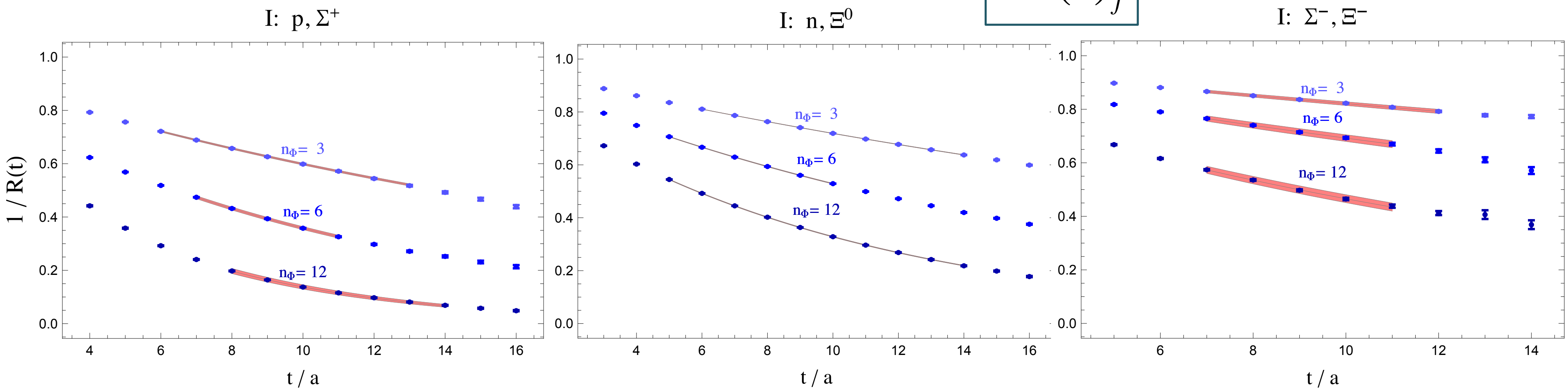

$$R_i(t) = \frac{G_i^{(+\frac{1}{2})}(t, n_\Phi)}{G_i^{(-\frac{1}{2})}(t, n_\Phi)} \Bigg/ \frac{G_i^{(+\frac{1}{2})}(t, 0)}{G_i^{(-\frac{1}{2})}(t, 0)}$$

$$\frac{1}{R_i(t)} \xrightarrow{t\to\infty} Z e^{-\delta E^B t}$$

$$q_d = q_s \Rightarrow \begin{pmatrix} u \\ d \\ s \end{pmatrix} \to \begin{pmatrix} 1 & 0 & 0 \\ 0 & \multicolumn{2}{c}{U} \\ 0 & & \end{pmatrix} \begin{pmatrix} u \\ d \\ s \end{pmatrix}$$

$U \in SU(2)$

LQCD calculations of magnetic moments

NPLQCD, PRD95, 114513 (2017)

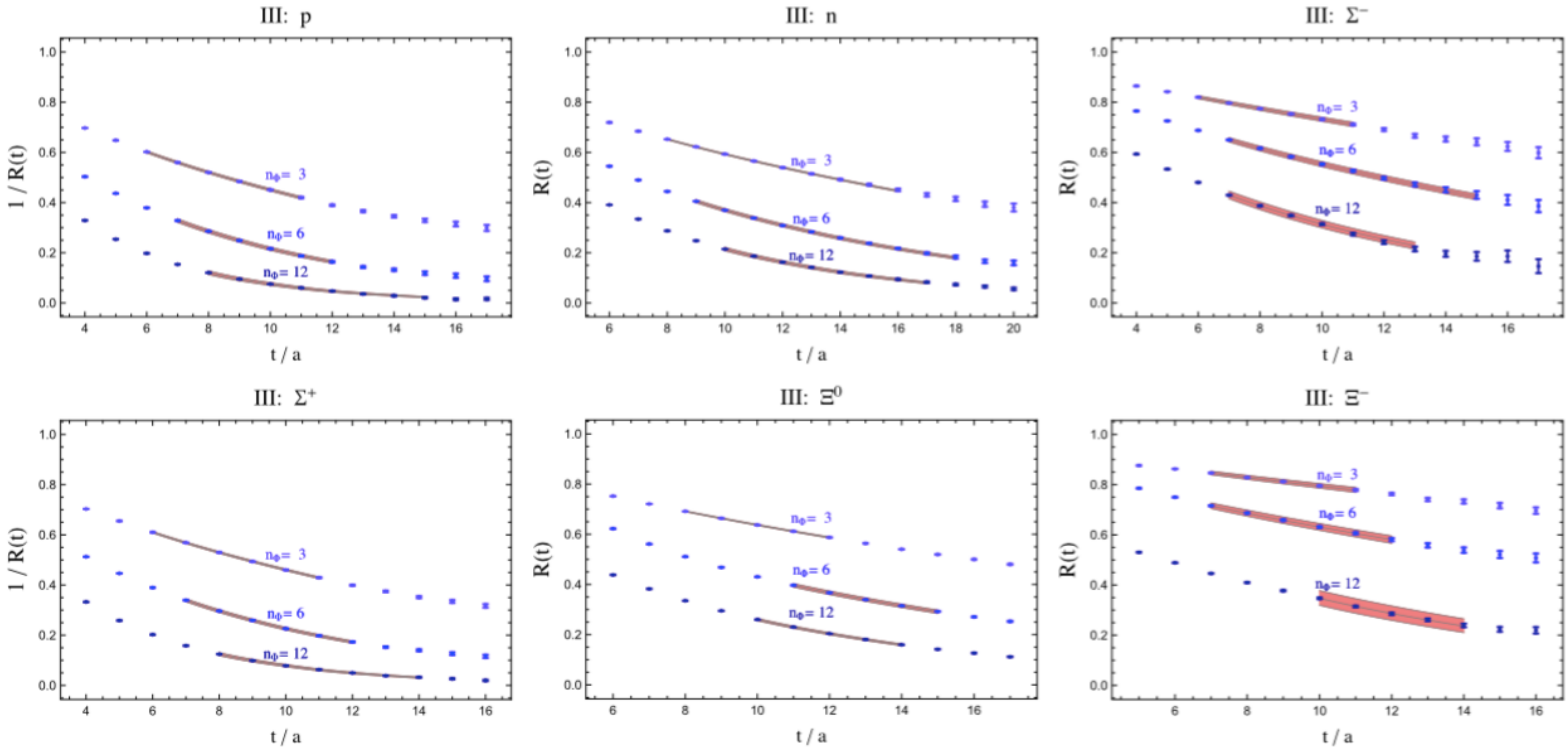

	L/a	T/a	β	am_l	am_s	a[fm]	m_π[MeV]	N_{cfg}
III	32	96	6.1	−0.2800	−0.2450	0.1167(16)	449.9(4.6)	544

LQCD calculations of magnetic moments

NPLQCD, PRD95, 114513 (2017)

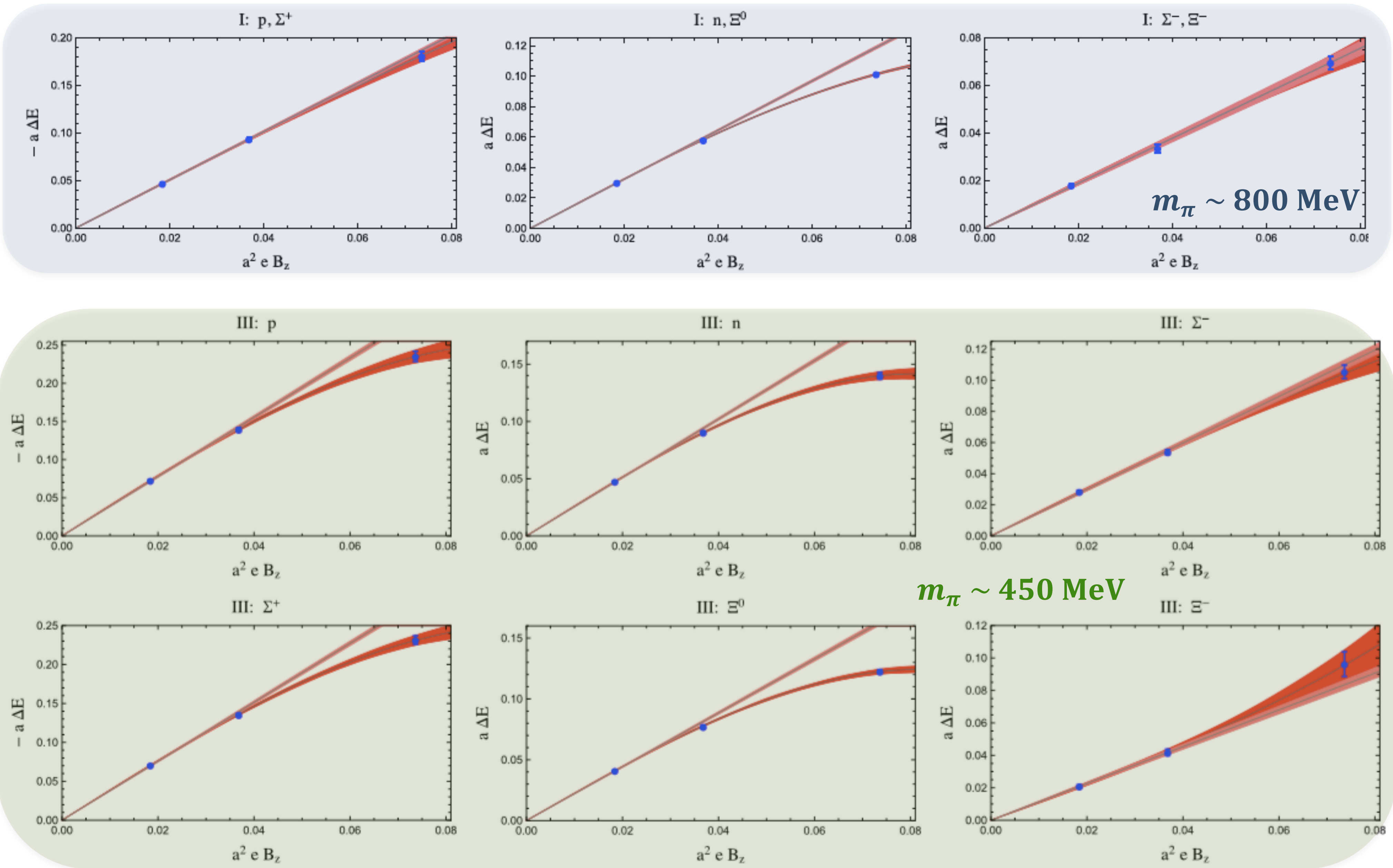

$$\delta E \equiv E_B^{(+1/2)}(\vec{B}) - E_B^{(-1/2)}(\vec{B}) = -2\,\mu_B\, B_z + \cdots$$

LQCD calculations of magnetic moments

NPLQCD, PRD95, 114513 (2017)

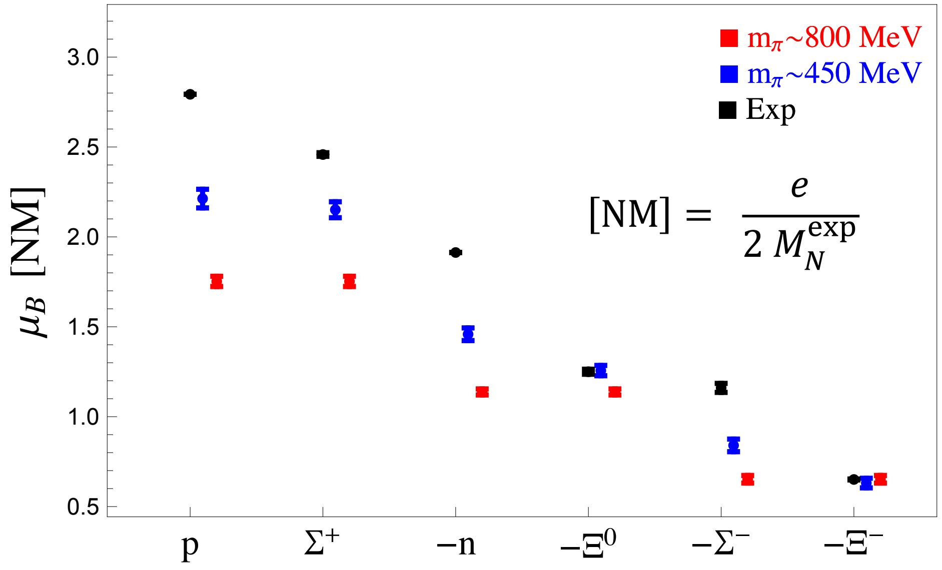

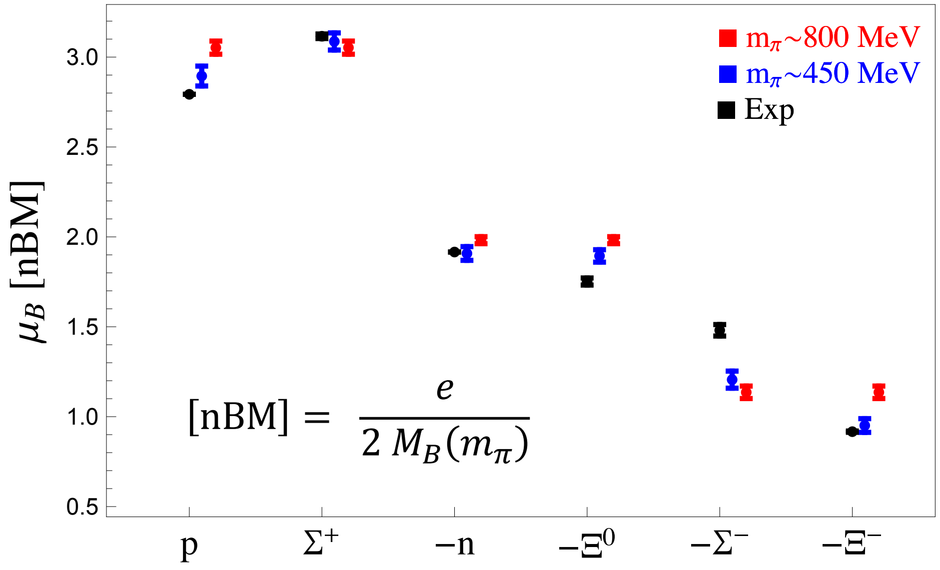

$(\mu_{-B} \equiv -\mu_B)$

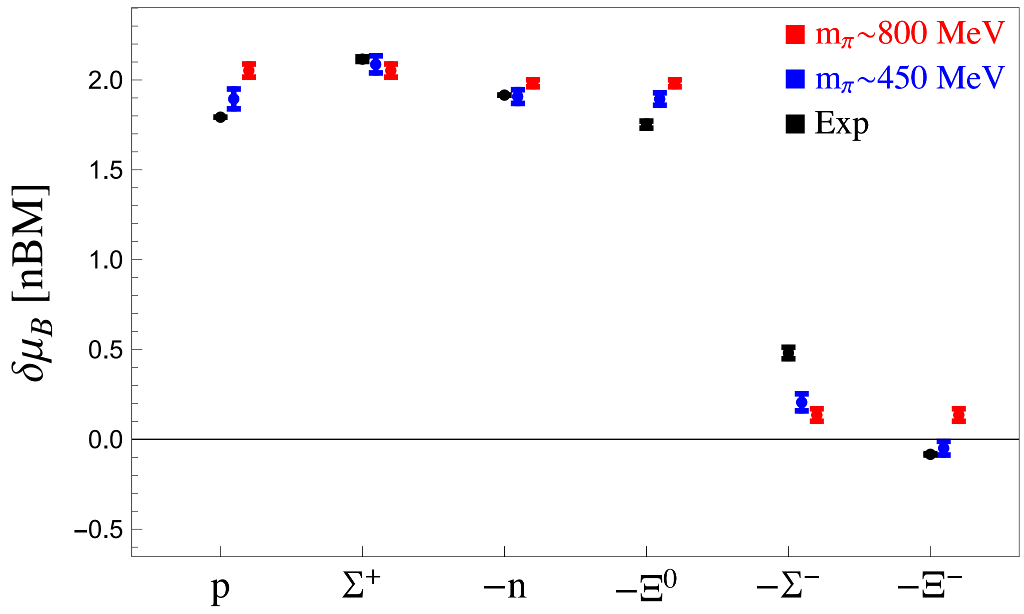

Dirac operator

$$\delta\mu_B[nBM] = \mu_B[nBM] - Q_B$$

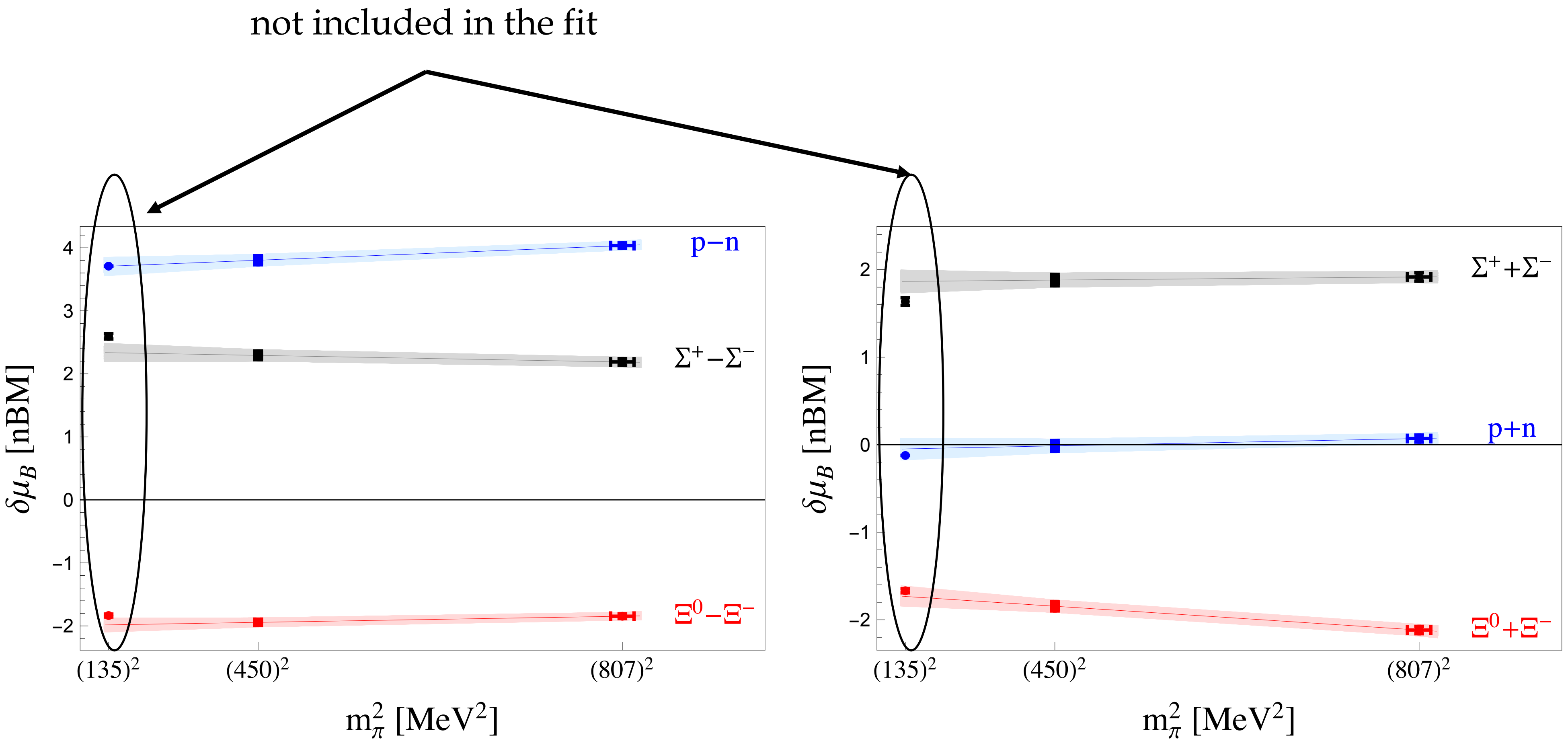

Quark mass extrapolation of the anomalous part of the isovector and isoscalar magnetic moments assuming

$$\delta\mu_B^I(m_\pi^2) = \delta\mu_B^I(0) + A_B^I m_\pi^2$$

NPLQCD, ongoing

1. ***Computation of heavier nuclei. In collaboration with A. Lovato (INFN-TIFPA)***

Extend the domain of LQCD predictions to heavier nuclei in a model-independent way

$\not{\pi}$ EFT → fit of LECs to LQCD calculations for few-baryon systems
+ QMC techniques

2. ***Analysis of YN and YY results from the 450 MeV pion mass calculation***

3. ***Continue production at lighter pion mass (~300 MeV)***